Carcinogenesis, 2022, **43**, 1149–1161
https://doi.org/10.1093/carcin/bgac083
Advance access publication 28 October 2022
Original Article

Original Article

RAS oncogene signal strength regulates matrisomal gene expression and tumorigenicity of mouse keratinocytes

Christophe Cataisson[1], Alex J. Lee[1], Ashley M. Zhang[1], Alicia Mizes[1], Serena Korkmaz[1], Brandi L. Carofino[1], Thomas J. Meyer[2,3], Aleksandra M. Michalowski[1], Luowei Li[1] and Stuart H. Yuspa[1,*]

[1]Laboratory of Cancer Biology and Genetics, National Cancer Institute, Bethesda, MD 20892, USA
[2]CCR Collaborative Bioinformatics Resource, National Cancer Institute, National Institutes of Health, Bethesda, MD, USA
[3]Advanced Biomedical Computational Science, Frederick National Laboratory for Cancer Research, Frederick, MD, USA

*Corresponding author: Laboratory of Cancer Biology and Genetics, Center for Cancer Research, National Cancer Institute, 37 Convent Drive, MSC-4255, Building 37, Room 4068, Bethesda, MD 20892-4255, USA. Tel: +301-480-8474; Fax: 240-541-4464Email: yuspas@mail.nih.gov

Abstract

Environmental and molecular carcinogenesis are linked by the discovery that chemical carcinogen induced-mutations in the *Hras* or *Kras* genes drives tumor development in mouse skin. Importantly, enhanced expression or allele amplification of the mutant *Ras* gene contributes to selection of initiated cells, tumor persistence, and progression. To explore the consequences of *Ras* oncogene signal strength, primary keratinocytes were isolated and cultured from the *LSL-Hras*^{G12D} and *LSL-Kras*^{G12D} C57BL/6J mouse models and the mutant allele was activated by adeno-Cre recombinase. Keratinocytes expressing one (H) or two (HH) mutant alleles of *Hras*^{G12D}, one *Kras*^{G12D} allele (K), or one of each (HK) were studied. All combinations of activated *Ras* alleles stimulated proliferation and drove transformation marker expression, but only HH and HK formed tumors. HH, HK, and K sustained long-term keratinocyte growth *in vitro*, while H and WT could not. RNA-Seq yielded two distinct gene expression profiles; HH, HK, and K formed one cluster while H clustered with WT. Weak MAPK activation was seen in H keratinocytes but treatment with a BRAF inhibitor enhanced MAPK signaling and facilitated tumor formation. K keratinocytes became tumorigenic when they were isolated from mice where the *LSL-Kras*^{G12D} allele was backcrossed from the C57BL/6 onto the FVB/N background. All tumorigenic keratinocytes but not the non-tumorigenic precursors shared a common remodeling of matrisomal gene expression that is associated with tumor formation. Thus, RAS oncogene signal strength determines cell-autonomous changes in initiated cells that are critical for their tumor-forming potential.

Graphical Abstract

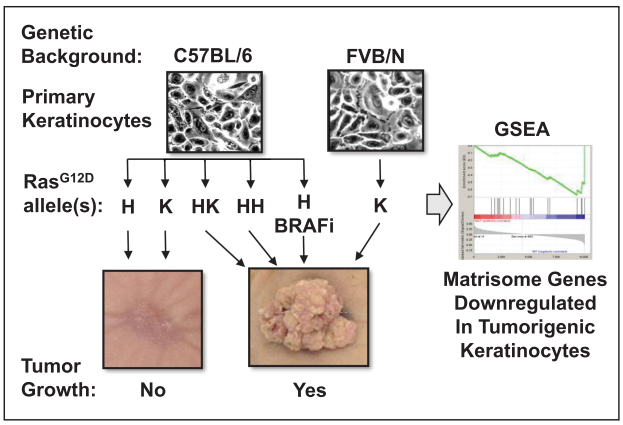

Introduction

Chemical carcinogenesis has been used for decades to define the driver mutations underpinning cancer initiation. Remarkably, when applied to mouse skin, the mutagens 7,12-dimethybenzo(a) anthracene (DMBA), *N*-methyl-*N*-nitrosurea (MNU), and methylcholanthrene (MCA) all result in premalignant papillomas bearing *Hras* activating mutations (1). The full tumor-initiating capacity of oncogenic *Hras* was confirmed when skin tumors erupted *in vivo* after the introduction of oncogenic *v-Hras* into keratinocytes (2,3). While carcinogen treatment

Received: April 27, 2022; Revised: October 3 2022; Accepted: October 27, 2022

is sufficient to induce *Hras* mutations in skin keratinocytes, homeostatic disruption by non-mutagenic tumor promoters is required for clonal expansion of initiated keratinocytes and tumor formation. Even then, between 20 and 50% of benign papillomas with confirmed *Hras* mutations regress when promoter treatment is stopped (4,5). Molecular studies on persistent papillomas suggest that expression of the *Hras* transcript is elevated by tumor promoters (6) or oncogene dosage is modified by selective trisomy of chromosomes 6 and 7 that carry the *Hras* and *Kras* genes (7). Alternatively, the *Hras* mutant allele could be selectively amplified at the benign stage (8). While mutations in *Hras* are frequently detected in carcinogen-initiated skin tumors, *Kras* mutations also drive papilloma formation in mouse skin and *Kras*-driven tumors tend to be larger and more persistent (9–11). Thus, the qualitative and quantitative properties of the individual mutant *Ras* alleles determine the destiny of tumors that develop in experimental cutaneous carcinogenesis. However, a dissection of the allele-specific downstream signaling that contributes to this destiny has not been performed.

The three *Ras* genes (*Hras*, *Kras*, and *Nras*) encode four RAS protein isoforms that are highly similar in primary sequence, structure, and biochemical properties. However, there are striking cancer-type specific mutational profiles of *RAS* gene isoforms in human cancer (12,13), with *KRAS* being mutated in one-third of all cancers. In mouse models, wild-type *Hras* and *Kras* are mostly bioequivalent, but their oncogenic counterparts display differential transforming properties (14,15). Some of those differences can be attributed to variation in expression level, signal intensity, and cellular context (16). Early transgenic models utilized constitutively active *Hras* overexpression to drive skin carcinogenesis (17,18), but newer knock-in approaches allow for constitutive expression of mutant *Hras* and *Kras* from their endogenous promoters, therefore bypassing the caveat of overexpression (19,20) and their application to mouse skin carcinogenesis studies (21).

Our past work has sought to understand how activating mutations in *Ras* are sufficient to initiate cancer in keratinocytes and produce the initiated phenotype that is manifested, through tumor promoter-induced clonal expansion, as the benign squamous papilloma. We have focused on a signaling cascade in which RAS activation establishes a series of autocrine loops through EGFR, IL-1R, NF-κB, and CXCR2 to produce hyperproliferation, delayed terminal differentiation, enhanced migration, and the elaboration of multiple chemokines and cytokines that are hallmarks of initiated keratinocytes. Interruption of any of these interacting pathways reduces or prevents tumor formation (11,22–24). In the current work, we used primary keratinocytes expressing one or multiple alleles of mutant *Hras* and mutant *Kras* expressed from their endogenous loci to track downstream effectors that might distinguish pathways that underlie the allele-specific differences in their transforming capabilities. In keeping the mutation identical (G12D) across comparisons, we have identified key differences among *Hras* and *Kras* mutants and the need for more than one mutant allele to be expressed for autonomous tumor formation to occur *in vivo*.

Materials and methods

Animals

LSL-Hras^{G12D} mice (stock #009046), *LSL-Kras*^{G12D} mice (stock #008179) (19) on a C57BL/6 genetic background and Rosa26-Cas9 knock-in mice on a FVB genetic background (stock# 026558) (25) were purchased from The Jackson Laboratory.

Cell culture and treatments

Primary mouse keratinocytes and hair follicle buds were isolated from newborn pups as described previously (26) and cultured in modified Eagle's medium (EMEM, Lonza 06-174G), 8% Chelex-treated FBS (Gemini Bio Products 100–106), and 0.05 mmol/L calcium unless otherwise indicated. The Cre recombinase (Cre) was introduced into primary keratinocytes using an adenoviral construct driven by a cytomegalovirus promoter. Keratinocytes were adenovirus-infected for 30 min in serum-free medium with a MOI of five viral particles per cell and hexadimethrine bromide (4 μg/mL, Sigma, 107689) to enhance uptake. Serum-containing medium was added to the cells for the next 48 h after the infection in the presence of the Rho-associated protein kinase inhibitor Y-27632 at 2.5 μM (Tocris) to limit the toxicity associated with the adenoviral transduction (27). Long-term cultures were fixed and stained with a 10% formalin/0.5% crystal violet solution.

Athymic nude mouse grafting

Mouse experiments were performed under a protocol approved by the National Cancer Institute (NCI) and National Institutes of Health Animal Care and Use Committee. Seven days after adenoviral Cre transduction, 7 million H, K, HH, or HK keratinocytes were mixed with 4 million SENCAR mouse primary dermal fibroblasts (cultured for 1 week) and grafted onto the back of nude mice on a prepared skin graft site located in the interscapular region (26). Tumor formation was monitored weekly for up to 8 weeks. Tumors were harvested, fixed in formalin and embedded in paraffin for hematoxylin and eosin (H&E) staining (Histoserv, Gaithersburg, MD).

RNA isolation and RNA-seq

RNA was isolated from cultured cells using RLT RNeasy 96 Qiacube HT Kit (Qiagen, 74171) and on-column DNA digest (Qiagen, 79254). The concentration of RNA was determined using a NanoDrop and the RNA integrity was analyzed with an RNA nanochip on a Bioanalyzer (Agilent Technologies, Santa Clara, CA). RNA samples were pooled and sequenced on 4 lanes of HiSeq3000 with Illumina HiSeq 3000/4000 chemistry. All the samples had yields above 96 million reads. RNA-seq data were aligned and counted using the CCR Collaborative Bioinformatics Resource (CCBR) in-house pipeline (https://github.com/CCBR/Pipeliner). Briefly, reads were trimmed of low-quality bases and adapter sequences were removed using Cutadapt v1.18. Mapping of reads to reference Mouse mm10 genome was performed using STAR v2.6.1 in 2-pass mode. Then, RSEM v1.2.31 was used to quantify gene-level expression, with counts normalized to library size as counts-per-million. Downstream analysis and visualization were performed within the NIH Integrated Analysis Portal (NIDAP) using R programs developed on the Foundry platform (Palantir Technologies). Here, quantile normalization and differential expression of genes analysis were performed using limma-voom v3.34.5 (28). Genes that were both significantly differentially expressed relative to control (adjusted $P < 0.01$) and that had absolute fold-changes relative to control ≥ 2.0 were retained for further analysis. Gene

set enrichment analysis (GSEA) was performed against four gene set collections (C6: Oncogenic signatures, CP: KEGG: KEGG gene sets, CP: Canonical pathways, and H: hallmark gene sets) from the Molecular Signatures Database (MSigDB version 6.2), using R and Bioconductor fgsea library version 1.8.0. Results were filtered based on adjusted *P*-value then sorted on Normalized Enrichment Score (NES). The data discussed in this publication have been deposited in NCBI's Gene Expression Omnibus and are accessible through GEO Series accession GSE200607 and GSE200632.

Statistical analysis

Unless otherwise specified, biochemical data were analyzed by Prism software, and significance values were assigned using the Mann–Whitney *U* test, Student's *t*-test, or one-way ANOVA with Dunnett's post-hoc test. Statistical significance of *P* values in figures are represented as follows: $*P \leq 0.05$, $**P \leq 0.01$, $***P \leq 0.001$.

Results

Mutant *Ras* genes have allele-specific effects on mouse keratinocytes

To explore the qualitative and quantitative molecular requirements for RAS signaling to produce autonomous tumor formation, we intercrossed *LSL-Hras*^{G12D} and *LSL-Kras*^{G12D} mice to generate a source of primary keratinocytes expressing either wild-type (WT) endogenous alleles, a single mutant allele (*Hras*^{G12D} or H, *Kras*^{G12D} or K), or two mutant alleles (*Hras*^{G12D} and *Kras*^{G12D} or HK). In parallel, we also intercrossed *LSL-Hras*^{G12D} animals to produce offspring expressing two *Hras*^{G12D} mutant alleles (or HH) (Supplementary Figure S1, available at *Carcinogenesis* Online). All mice were on a C57BL/6 background. After establishing primary keratinocyte cultures from newborn mice, we transduced cultures with an adenovirus expressing Cre recombinase to delete the LSL cassette(s) and allow expression of mutant *Ras*. Proper expression of WT and mutant alleles of each genotype was confirmed by digital droplet PCR (Supplementary Figure S2A and B, available at *Carcinogenesis* Online). This analysis also revealed that expression of one *Kras*^{G12D} allele in K and HK reduced the expression of the *Kras*^{WT} allele by half when compared to WT, H, and HH (Supplementary Figure S2A, available at *Carcinogenesis* Online). Likewise, expression of *Hras*^{G12D} reduced the expression of *Hras*^{WT} by half (Supplementary Figure S2B, available at *Carcinogenesis* Online). Unexpectedly expression of the mutant *Kras* allele also reduced the expression of the *Hras*^{WT} allele.

To directly test the tumor-forming abilities of H, K, HH, and HK keratinocytes, we employed an orthotopic grafting assay in nude mice (26). Seven days after adenoviral Cre treatment, keratinocytes were harvested and transplanted to a prepared orthotopic graft site in the adipose-rich and highly vascular interscapular region, a site that we reported to be the most permissive for tumor formation (24). Under these conditions, only keratinocytes expressing two mutant alleles (HH and HK) formed squamous papillomas (Figure 1A). A hallmark of keratinocyte transformation by *v-Ras*^{Ha} transduction is hyperproliferation, which was replicated by all endogenous mutant *Ras* combinations independent of their differences in tumor formation (Figure 1B). Untreated cultured keratinocytes undergo terminal differentiation or senescence and detach after several weeks. After 11 days, our cultures remained confluent irrespective of *Ras* allele combination (Figure 1C). However, only the K, HK, and HH alleles, but not the single H allele, were able to maintain keratinocyte culture confluency for at least 30 days (Figure 1C), suggesting a strong negative influence on differentiation or senescence by these pathways. In the highly regulated stratification of the skin, only basal cells proliferate, but proliferation persists above the basal cell compartment in oncogenic *Ras*-induced papillomas. This can be modeled in keratinocyte cultures by switching cells from proliferation medium (0.05 mM calcium) to differentiating medium (0.5 mM calcium) and measuring proliferation (29). Under these circumstances, only K, HK, and HH alleles, but not the single H allele, supported continued proliferation in 0.5 mM calcium for 7 days (Figure 1D). The ability to maintain proliferation in a differentiation-inducing environment was consistent with the ability of HH and HK, but not H, keratinocytes to form tumors, but left the lack of tumor formation by K keratinocytes unexplained. Using an *in vitro* migration assay, we could demonstrate that all *Ras* alleles enhanced migration above wiltype keratinocytes but migration was further enhanced when comparing HH versus H and HK versus K (Figure 1E) suggesting that migration properties may contribute to potential for tumor formation as seen for keratinocytes expressing double mutant alleles from their respective control.

Mutant *Hras*^{G12D} and *Kras*^{G12D} signaling outputs are not equal in primary keratinocytes

We next performed molecular analyses to dissect the mechanism(s) underpinning the tumorigenicity of keratinocytes expressing different *Ras* alleles. Immunoblot analysis indicated that either one or two mutant *Ras* alleles activated MAPK signaling in all four genotypes, whereas a single *Hras* allele showed the weakest activation (Figure 2A) as measured by phospho-MEK and phospho-ERK. Since MAPK activation in keratinocytes is a consequence of both the expression of constitutively active RAS and autocrine activation of upstream EGFR (30), the strong increase in EGFR Tyr1068 phosphorylation in K, HH, and HK keratinocytes relative to H paralleled the other markers. As suggested by the droplet PCR, the activation of the K allele in K or HK reduced the expression of the endogenous WT HRAS protein to a small degree. pAKT was not different across the genotypes. Probing nuclear extracts for key transcription factors downstream of oncogenic RAS showed a very strong increase in nuclear phosphorylated FOSL1, particularly for the double mutants and K, but not for H. Nuclear phosphorylated c-Jun was also increased for all mutants. Nuclear residence of NF-κB p65 and RelB was detected in all genotypes, consistent with previous findings in *v-Ras*^{Ha} in keratinocytes (24). DNp63, which has been associated with papilloma formation and progression (31), was increased in the nuclear fraction of all *Ras* genotypes except for HH. Further, IκBζ, which we previously associated with *v-Hras*^{Ha} transformation of keratinocytes (32), showed increased nuclear residence with all mutant *Ras* alleles (Figure 2B). Together these results indicate that each individual mutant *Ras* allele configuration drives unique responses in pathways implicated in tumor formation, with the H allele having the weakest effects and the double mutants having the strongest.

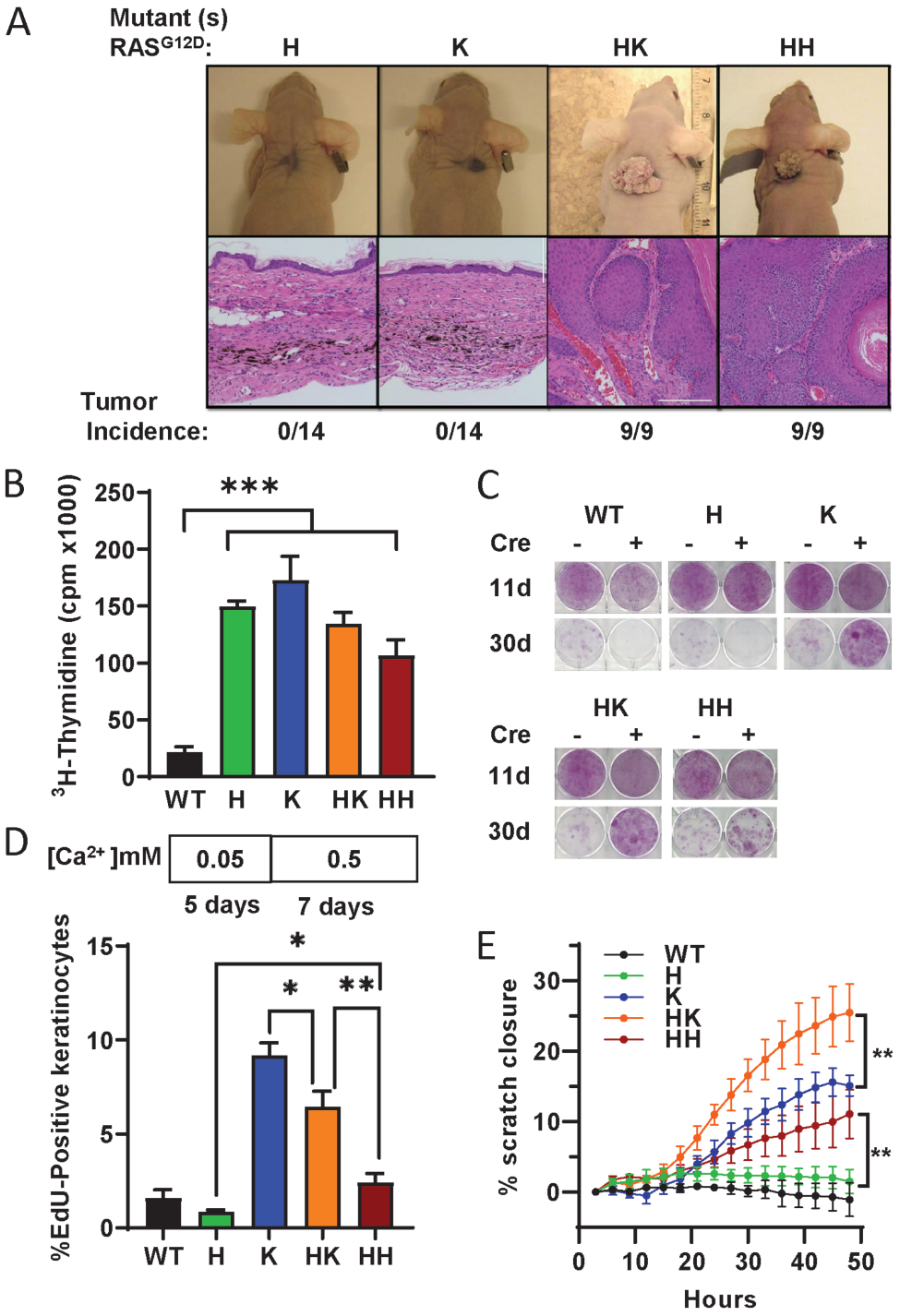

Figure 1. Only orthotopic grafts expressing two mutant alleles (HH or HK) produce squamous papillomas. (A) Representative photographs of orthotopic grafts at the interscapular site at collection time. WT, H, K, HK, and H keratinocytes, 7 days after transduction with Cre recombinase, were mixed with mouse primary dermal fibroblasts before grafting as described in the methods. Tumor incidence is indicated below the figure for each genotype and represent the compilation of multiple independent grafting experiments. 200 μm scale bar. (B) Tritiated thymidine incorporation was measured in WT, H, K, HK, and HH keratinocytes 7 days after transduction with Cre recombinase. (C) Cristal violet staining of long-term culture dishes (11 and 30 days) in the presence or absence of Cre recombinase treatment. (D) Timeline of culture conditions, WT, H, K, HK, and HH keratinocyte cultures were transduced with Cre and kept for 5 extra days under proliferative conditions (0.05 mM Ca^{2+}) then culture for 7 days under differentiating (0.5 mM Ca^{2+}) prior to EdU addition (arrowhead). (E) Incucyte scratch assay quantification on WT, H, K, HK, and HH keratinocyte cultures transduced with Cre and kept for 5 extra days under proliferative conditions followed by mitomycin treatment prior to the scratch assay.

The increased nuclear residence of FOSL1 and p65 by all oncogenic *Ras* alleles prompted us to examine their regulation of markers previously associated with keratinocyte transformation by *v-Ras*^{Ha} (24,33). CRISPR was used to separately ablate *Fosl1* and *Rela* in K keratinocytes (Supplementary Figure S3A, available at *Carcinogenesis* Online). Neither ablation reversed the suppression of the differentiation marker *Krt1* (Supplementary Figure S3B, available at *Carcinogenesis*

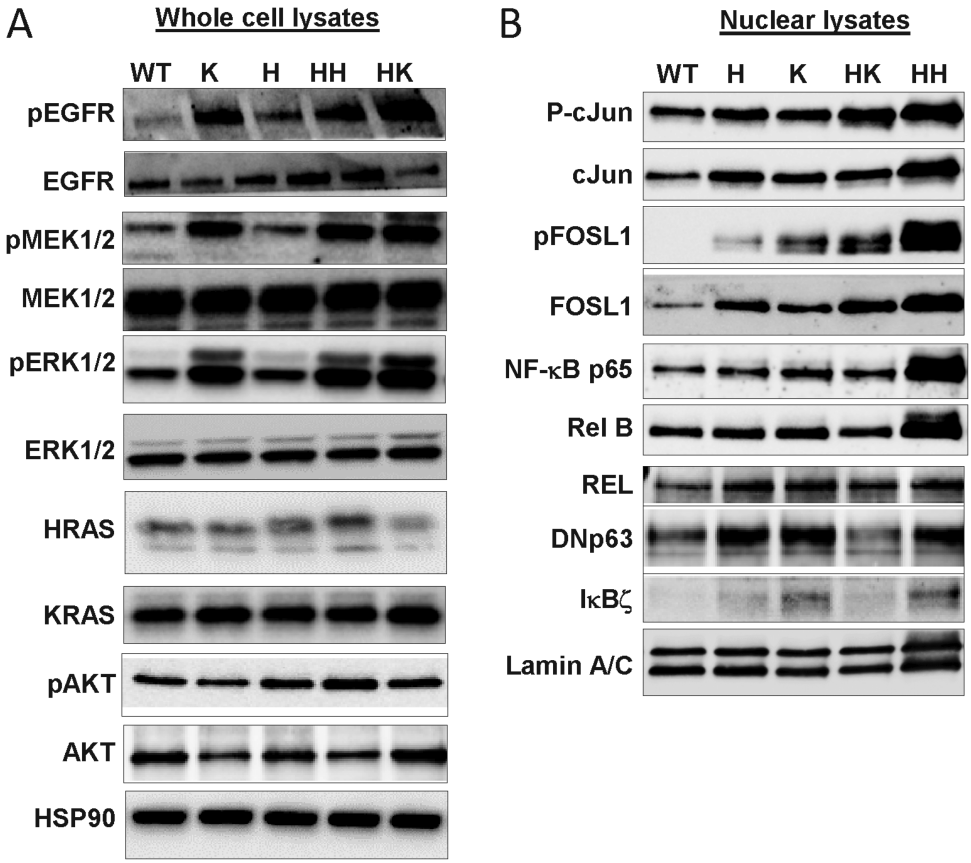

Figure 2. Mutant *Hras* and *Kras* exhibit different biological output in primary keratinocytes. (A) total cell extract and nuclear extracts (B) from WT, H, K, HK, and H keratinocytes 7 days after transduction with Cre were analyzed by immunoblotting for the indicated proteins. HSP90 and Lamin A/C were used as a loading control for cell lysates and nuclear extracts respectively.

Online). Loss of FOSL1 potentiated the expression of the cytokine *Cxcl1* and the EGFR ligand *Areg*, indicating that FOSL1 and its AP-1 partners are negative regulators of those genes. In contrast, both transcription factors were positive regulators of *Krt8*, a marker tied to papilloma progression *in vivo* (34). These results show that RAS controls transformation markers through specific transcriptional interactions suggesting that a broader transcriptional study could reveal profiles associated with tumor formation.

Non-tumorigenic K keratinocytes share gene expression profiles with tumorigenic keratinocytes

To further characterize if unique transcriptional changes could distinguish tumorigenic versus non-tumorigenic RAS genotypes, we subjected WT, H, K, HH, and HK keratinocytes to RNA sequencing analysis. Following unsupervised hierarchical clustering of the top 100 genes with the most variance among the five genotypes, two major distributions were revealed (Figure 3A). One gene distribution consisted of WT and H keratinocytes. The second distribution consisted of HH, K, and HK, with K clustering closest to HK despite not being able to form tumors *in vivo*. Volcano plots were generated to visualize differentially expressed genes across several pair-wise comparisons of tumorigenic versus non-tumorigenic groups containing a common mutant allele. Comparing tumorigenic HH to non-tumorigenic H keratinocytes and tumorigenic HK to non-tumorigenic K keratinocytes identified unique sets of differentially expressed genes, suggesting that there is no uniform transcriptomic change that determines tumor formation downstream of different mutant *Ras* alleles (Supplementary Figure S4, available at *Carcinogenesis* Online; Supplementary Table S1, available at *Carcinogenesis* Online). This was confirmed by the comparison of the two tumorigenic genotypes, HH and HK, where there were many differentially expressed genes. As depicted on the Venn diagram, 192 genes were shared by the HH versus H and HK versus K groups, while 577 and 207 were uniquely represented for each respective contrast (Figure 3B; Supplementary Table S2, available at *Carcinogenesis* Online).

To further understand the consequences for tumor formation by adding a second mutant *Ras* allele, we performed an in-depth analysis comparing HH versus H and HK versus K transcriptomes at the pathway level. Pre-ranked gene set enrichment analysis (GSEA) was performed and sets with adjusted *P*-values ≤ 0.01 were considered significantly perturbed; 68 and 38 gene sets were significantly perturbed in the HH versus H and HK versus K contrasts respectively (Supplementary Table S3, available at *Carcinogenesis* Online). Those gene sets were grouped according to four main processes/pathways (Figure 3C). The RAS/MAPK/AKT gene sets (blue) were enriched in HH and HK compared to their non-tumorigenic counterparts, reflecting the upregulation of RAS signaling upon the addition of a second mutated *Ras* allele. The same was also true for gene sets associated with NF-κB and inflammation (orange). Unexpectedly, gene sets associated with cell cycle (beige) tended to be negatively enriched in

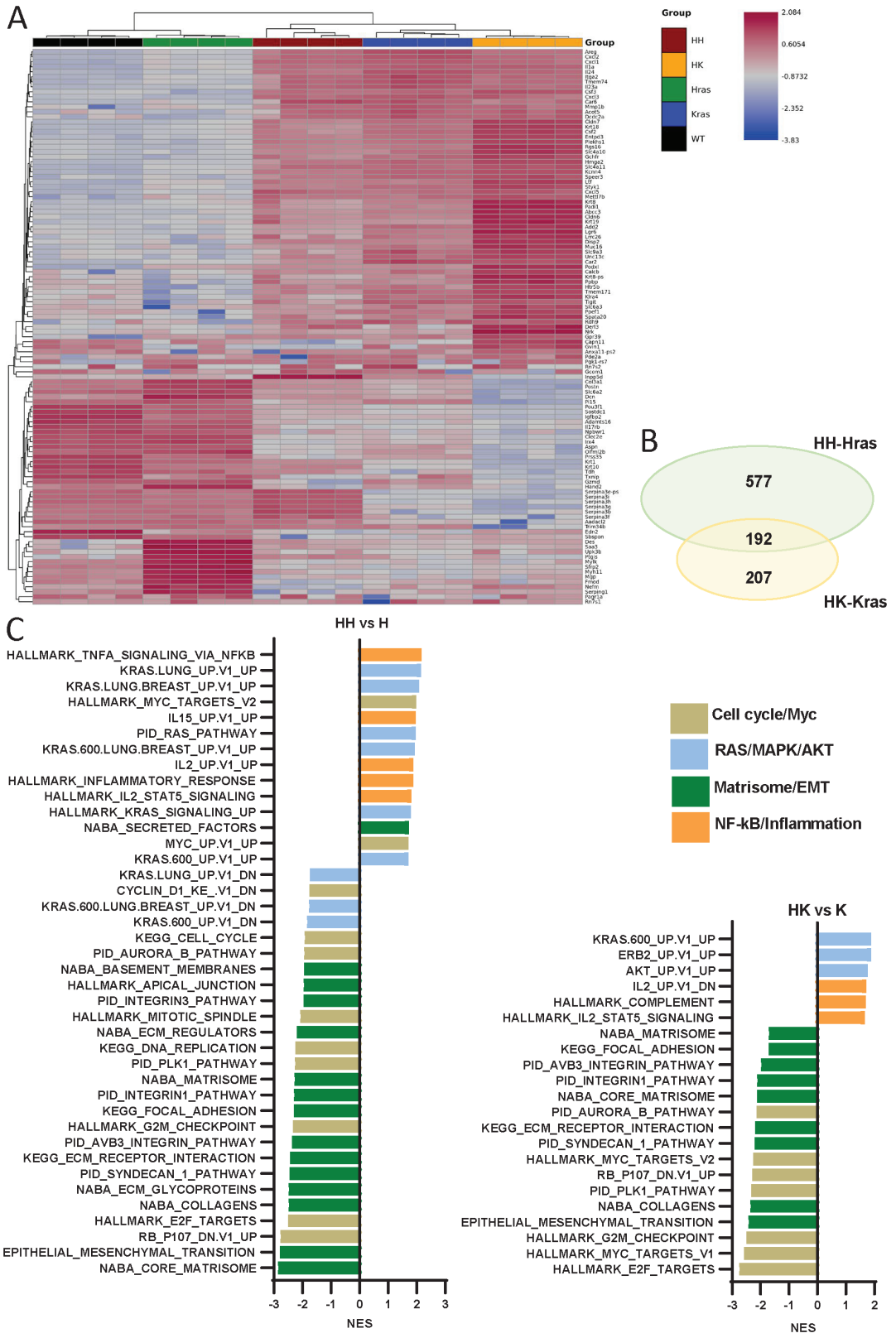

Figure 3. K keratinocytes despite being non-tumorigenic share a large gene signature with HK and HH keratinocytes. (A) Clustered heatmap of the 100 most variable genes, by expression, across all samples. (B) Venn diagram depicting the number of differentially expressed genes in the HK versus K and HH versus H keratinocytes. (C) GSEA analysis of pre-ranked gene sets with adjusted *P*-values ≤ 0.01 were plotted as a bar graph of NES (normalized enrichment score) and color coded according to their belonging to four main groups.

HK versus K and were mixed in HH versus H. Proliferation assays (Figure 1B) also indicated that double mutants did not proliferate more than single mutants, indicating that *in vitro* proliferation is not predictive of tumor formation capacity of keratinocytes *in vivo*. The largest number and most consistent gene sets negatively enriched in HH were related to the matrisome/epithelial-to-mesenchymal transition (EMT) group (green). The CORE_Matrisome collection contains genes encoding core extracellular matrix (ECM) components, including glycoproteins, collagens, and proteoglycans (35). The same collection of matrisome-related gene sets was also negatively enriched in HK compared to K (Figure 3C). Leading edge plots revealed the most differentially expressed genes contributing to the negative enrichment of the matrisome collection in double versus single mutants (Figure 4A). Notably, keratinocyte expression of multiple collagen genes and other ECM components (collagen 6, fibulin 5, slit 3, and thrombospondin2) were reduced in double mutants relative to the corresponding single mutant, suggesting that ECM remodeling by keratinocytes is critical for RAS-driven tumor formation. In contrast, expression of genes involved in basal cell attachment, such as α3, α6, and β1integrins, were elevated in the double mutants and K but not in H (Supplementary Figure S5, available at *Carcinogenesis* Online).

BRAF inhibitor treatment potentiated the signal strength and tumorigenicity of keratinocytes expressing a single mutant *Hras* allele

The work of Terell et al. has shown that the limited engagement of mutant HRAS with its downstream BRAF effector can be paradoxically overcome by treatment with a BRAF inhibitor (36). We asked if this treatment could alter the transformation profile and tumorigenicity of H keratinocytes. Indeed, treatment of H keratinocytes with the BRAF inhibitor PLX4720 potentiated the induction of *Areg, Krt8*, and *Dusp6* and accentuated the suppression of *Krt10* expression, all markers of enhanced mutant HRAS potency. (Figure 5A). Coordinately, activation of ERK was increased (Figure 5B) and EdU incorporation was slightly elevated in H keratinocytes treated with PLX4720 (Figure 5C) but the expression level of the $Hras^{G12D}$ allele was not changed by PLX4720 treatment (Figure 5D). Recovery from 7 days in differentiating conditions (0.5 mM calcium) to resume proliferation after 2 days in proliferation medium (0.05 mM calcium), a response associated with tumor formation, was very robust in PLX-treated H cultures relative to untreated H cells (Figure 5E). When PLX-treated H cells were orthotopically grafted to recipient nude mice treated with PLX at 20 mg/kg, papillomas formed in 2 of 5 recipient mice after 21 days (Figure 5F), suggesting that PLX enhanced the signaling output of a single mutant *Hras* allele to allow for tumor formation. RNA-seq and GSEA analysis to compare H-PLX vs H gene expression was performed with the same four collections used earlier (Supplementary Table S3, available at *Carcinogenesis* Online). The matrisome/EMT pathways were the most negatively enriched gene set collection associated with the BRAF inhibitor treatment (Supplementary Figure S6A, available at *Carcinogenesis* Online). Examination of a selected list of matrisome genes confirmed that the elevation to a tumorigenic phenotype by PLX treatment of H keratinocytes was also associated with their reduced expression (Supplementary Figure S6B, available at *Carcinogenesis* Online).

A single mutant *Kras* allele is tumorigenic when expressed on a permissive genetic background

The observation that K keratinocytes did not form tumors, yet clustered with the double mutants on the RNA-seq heatmap, presented a conundrum. The background strain from which keratinocytes are isolated strongly influences their neoplastic phenotype *in vitro* and their tumor forming potential *in vivo* as *de novo* tumors or orthografts (24,37,38). The C57BL/6 strain used here is the most suppressive. To address the possibility that the genetic background of K keratinocytes was suppressing tumor formation in orthografts, C57BL/6 *LSL-*$Kras^{G12D}$ mice were backcrossed for 1, 2, and 3 generations with the permissive FVB/N mouse strain. After activating the mutant K allele *in vitro*, keratinocytes were grafted to nude mice. Orthografts of N3 but not N1 or N2 keratinocytes formed squamous papillomas (Figure 6A). The expression level of the $Kras^{WT}$ and mutant $Kras^{G12D}$ allele did not differ in N1 or N3 K cultures of isolated keratinocytes (Figure 6B) nor did phospho-ERK (Figure 6C). RNA-seq and GSEA analysis of pre-ranked gene sets with adjusted *P*-values ≤ 0.01 were plotted as NES of N3 versus N1 monitoring the same four collections used earlier (Supplementary Table S2, available at *Carcinogenesis* Online). Cell cycle and Myc gene collections were positively enriched on the FVB background (N3 versus N1), while NF-κB and RAS/MAPK gene collections were negatively enriched (Figure 6D). As seen before, the matrisome/EMT pathways were the most negatively enriched gene set collection associated with the acquisition of tumorigenicity in N3 keratinocytes when compared to N1 (Figure 6D). Examination of leading-edge genes for the RAS/MAPK pathway (Supplementary Figure S7A and B, available at *Carcinogenesis* Online) illuminates the reduction in expression of genes such as *Dusp5*, *Dusp6,* and *Dusp9*, which are direct negative feedback regulators of MAPK signaling, and *Rasa1* and *Mapkapk3*, which integrate non-oncogenic signaling, suggesting decreased expression of genes that have an anti-oncogenic effect. Leading edge analysis of the ECM receptor interaction pathway identified familiar reductions in collagen genes and multiple laminin genes in the N3 versus the N1 K keratinocytes (Supplementary Figure S7B, available at *Carcinogenesis* Online). These results highlight the association between the downregulation of ECM-related genes and the tumorigenic potential of primary keratinocytes expressing mutant *Ras* allele(s).

Discussion

Amplification of a mutant *Hras* allele and upregulation of mutant *Hras* expression contribute to papilloma persistence and progression (6,8,39). We have previously modeled this using *v-*Ras^{Ha}-transformed primary mouse keratinocytes to elucidate individual cell-autonomous molecules and pathways whose deletion abrogates tumor formation. By this approach, we identified the essentiality of EGFR, IL-1, MyD88, and CXCR2 signaling either upstream or downstream from RAS for tumors to develop and a set of transformation-associated markers (amphiregulin, keratins 1, 10, 8, IL-1α, FOSL1, and CXCL1) (11,23,24,32). In the current study, we sought to extend our findings to a system where mutant *Ras* is expressed at physiological levels from endogenous loci, which more closely reflects the pathological state of oncogenic RAS-transformed cells as they exist *in situ* in initiated

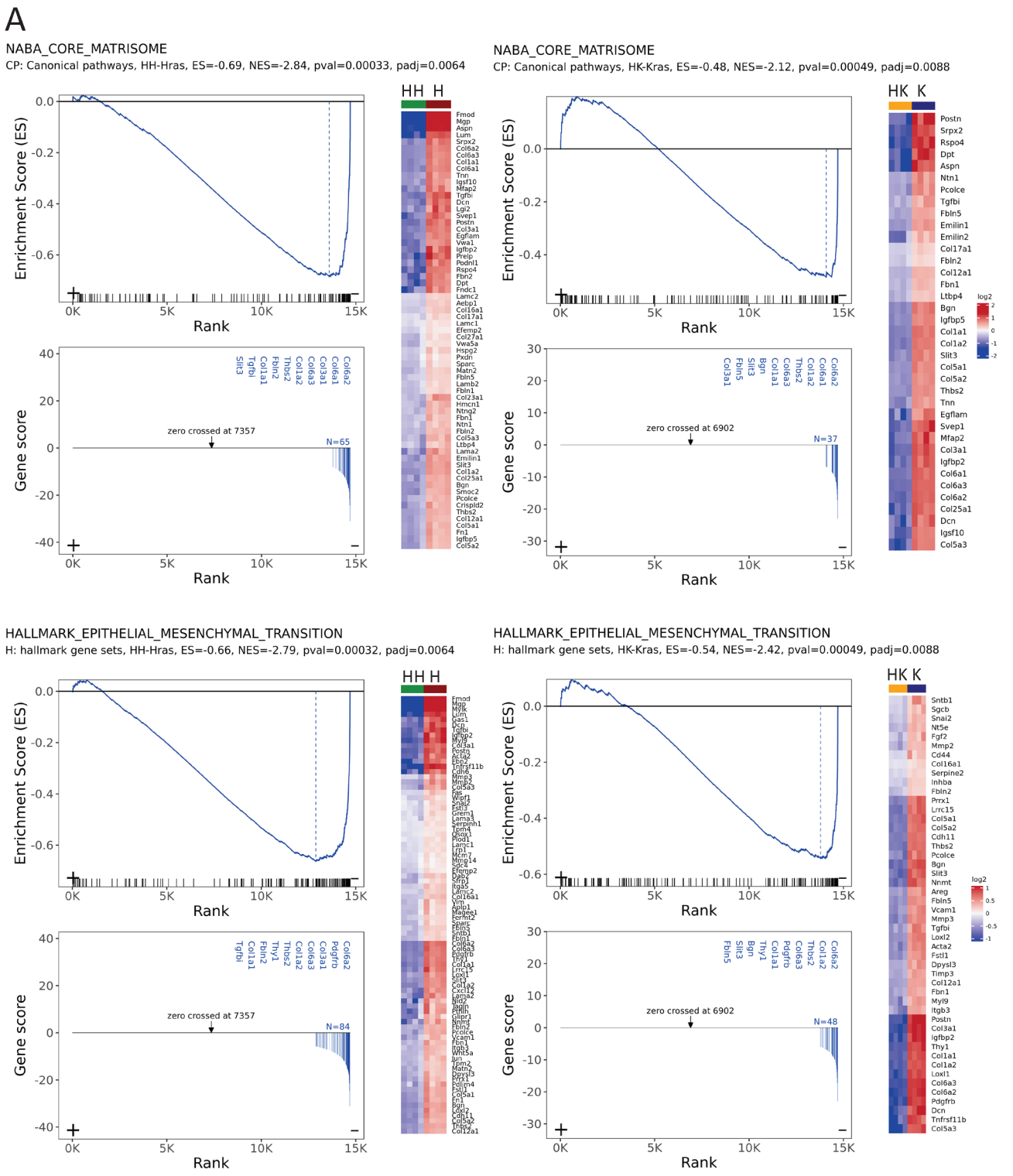

Figure 4. Gene sets related to matrisome and EMT are concordantly downregulated in HH versus H and HK versus K datasets. Plots of actual enrichment results for the NABA CORE MATRISOME and Hallmark EPITHELIAL MESENCHIMAL TRANSITION (EMT) gene sets against the HH versus H (left) and HK versus K (right) datasets. Heatmaps represent the leading-edge genes identified in GSEA analysis. Top 10 leading edge genes are listed in blue for each plot.

skin. We used keratinocytes isolated from C57BL/6 mice with a conditional oncogenic *Kras* or *Hras* knock-in allele to perform orthotopic grafting and molecular studies to test tumor forming potential and identify pathways associated with the acquisition of tumorigenicity.

Increased oncogenic RAS signal strength remodels the keratinocyte matrisome

Oncogenic signal strength was a prerequisite for cell-autonomous tumor formation; only keratinocytes bearing two mutant knock-in alleles (HH or HK) or some other form

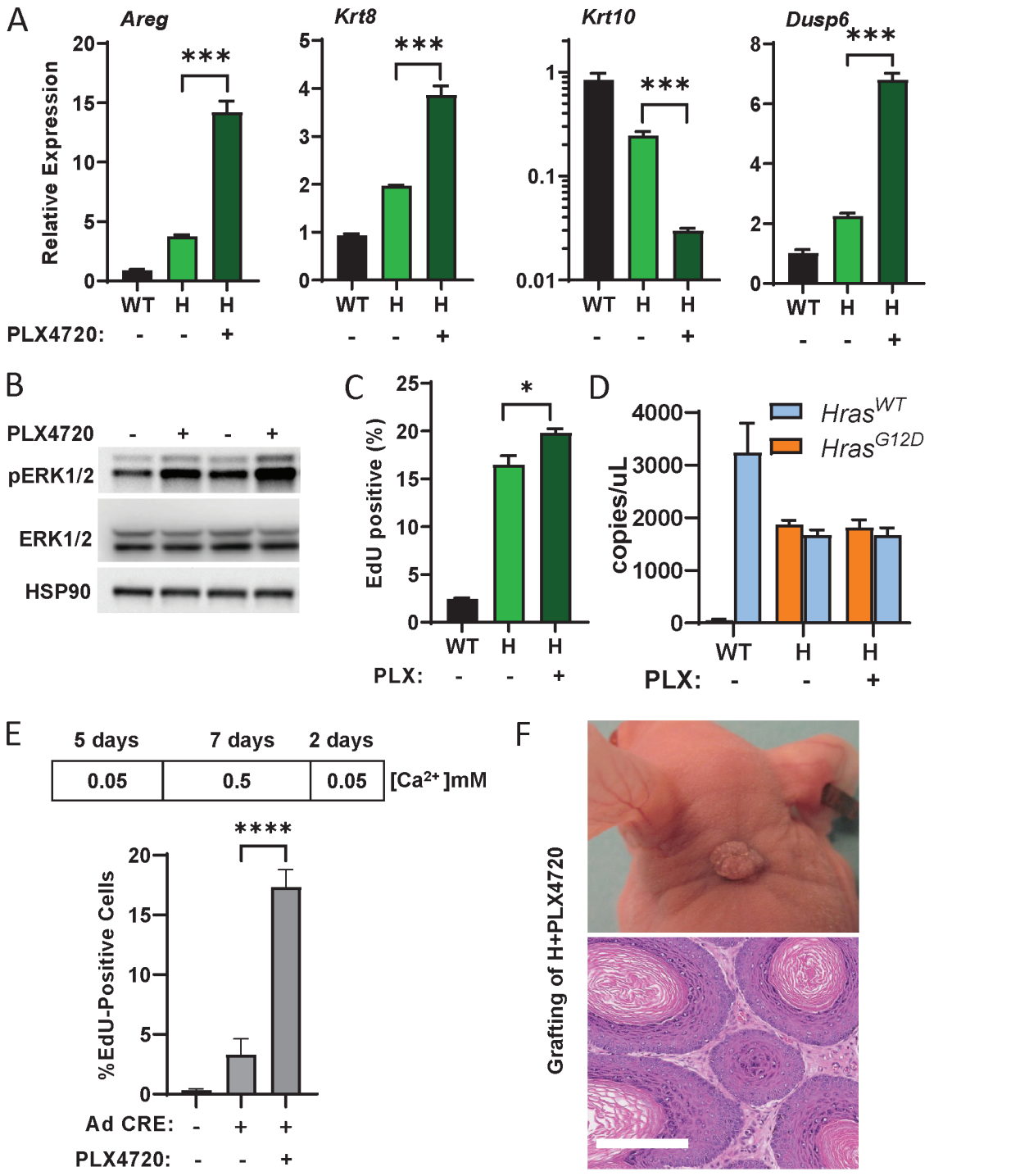

Figure 5. Treatment of H keratinocytes with a BRAF inhibitor strengthen mutant *Hras* biological output allowing for papilloma formation. (A) Real-time PCR analysis of amphiregulin (*Areg*), keratin 8 (*Krt8*), keratin 10 (*Krt10*), and Dual Specificity Phosphatase 6 (*Dusp6*) mRNA expression in WT and H keratinocytes cultures transduced with Cre for 5 days followed by 24 h treatment with the BRAF inhibitor PLX4720. (B) Western blot analysis of total cell extract from WT and H cultures treated for 24 h with PLX4720. (C) EdU incorporation was measured under the same conditions described in A. (D) Quantification of a *Hras* WT and *Hras* mutant (G12D) mRNA expression using droplet digital PCR. (E) Timeline of culture conditions H keratinocyte cultures were transduced with Cre and kept for 5 extra days under proliferative conditions (0.05 mM Ca^{2+}) then culture for 7 days under differentiating (0.5 mM Ca^{2+}) and returned to proliferative conditions (0.05 mM Ca^{2+}) for 2 days prior to EdU addition. (F) Top, Representative photograph of orthotopic graft at the interscapular site at collection time. H keratinocytes, 7 days after transduction with Cre recombinase and concomitantly treated with PLX4720, were mixed with mouse primary dermal fibroblasts before grafting as described in the methods. Bottom, H&E staining of resulting squamous papilloma. Scale bar is 200 μm.

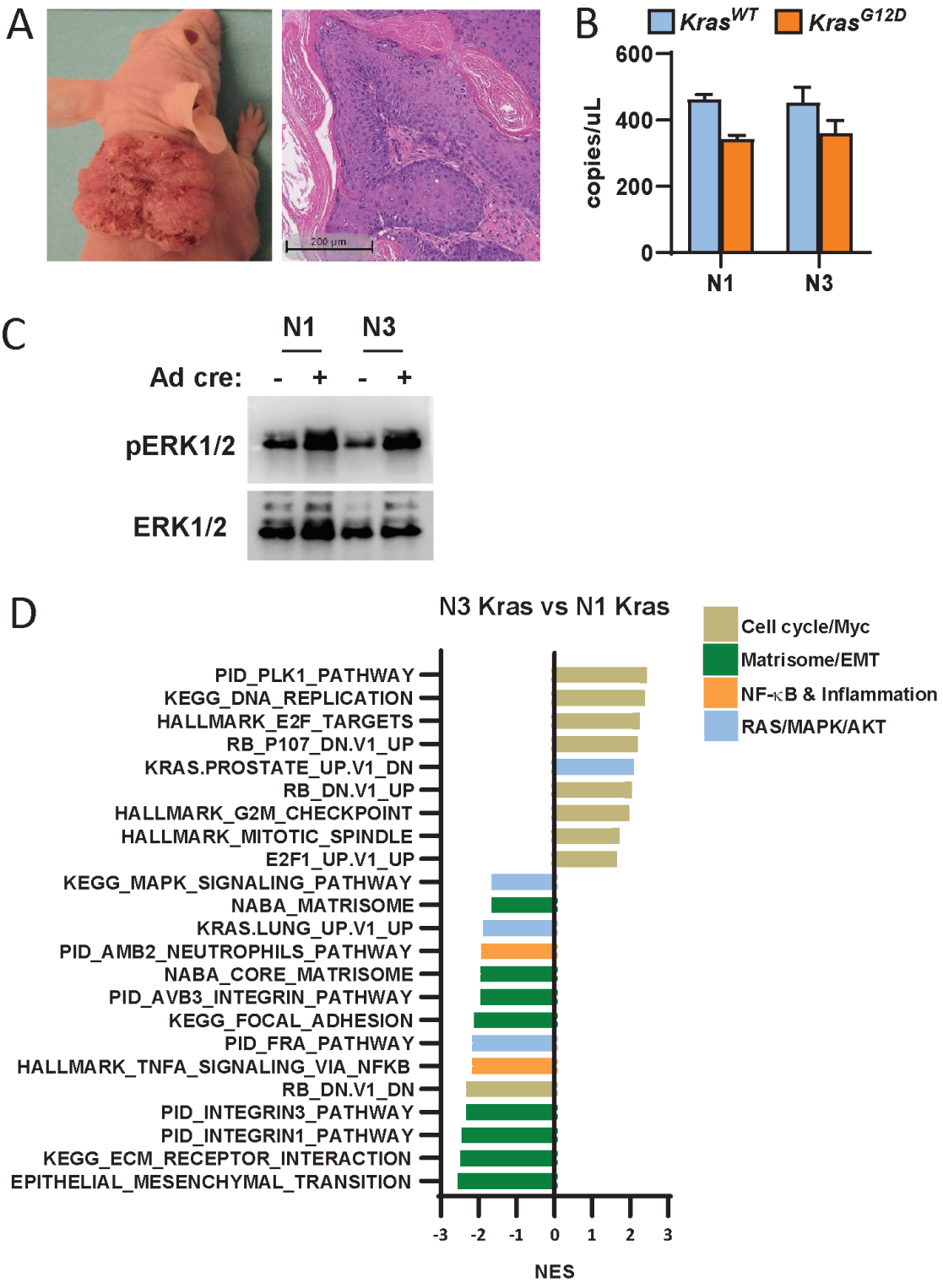

Figure 6. A permissive genetic background allows tumor formation driven by a single *Kras* mutant allele. (A) Left, Representative photograph of orthotopic graft at the interscapular site at collection time. K keratinocytes, 7 days after transduction with Cre recombinase were mixed with mouse primary dermal fibroblasts before grafting as described in the methods. Right, H&E staining of resulting squamous papilloma. Scale bar is 200 µm. (B) Quantification of a *Kras* WT and *Kras* mutant (G12D) mRNA expression using droplet digital PCR. (C) Total cell extract N1 and N3 keratinocytes 7 days after mock transduction (–) or Cre transduction (+) were analyzed by immunoblotting for the indicated proteins. (D) GSEA analysis of pre-ranked gene sets with adjusted *P*-values ≤ 0.01 were plotted as a bar graph of NES (normalized enrichment score) and color-coded according to their belonging to four main groups when comparing N3 versus N1.

of H or K signal amplification formed tumors. Interestingly, *in vitro* RAS-mediated stimulation of proliferation was not predictive of *in vivo* tumorigenicity. Transcriptional profiling also yielded clustering that placed K keratinocytes, though not tumorigenic, with the tumorigenic HH and HK groups. Surprisingly, the most distinguishing parameter that coincided with tumor formation among the groups was reduced expression of a cohort of genes that encode components of the ECM (matrisome). While the ECM components produced and secreted by keratinocytes are complex, our results are particularly noteworthy for the association of tumor formation with the double *Ras* mutants and reduction in transcripts for certain collagen components (*Col6a1*, *Col6a2*, *Col6a3*, *Col1a1*, *Col1a2*, and *Col3a1*) and other matrisome components (*Thbs2*, *Fibln5*, and *Bgn*) as compared with the H or K single mutants. We previously reported a unique reduction in expression of the proteinaceous ECM gene collection in tumorigenic keratinocytes transformed by activated MET, which engages the RAS pathway through activation of EGFR (11). Others have reported RAS/MAPK-driven reductions in expression of matrisomal genes, including *Col8a2*, *Col4a1*, *Serpinb4*, *Serpinb9*, *Lama5* and others, in mammary tumor cells that is associated with enhanced tumor growth (40). The composition of the matrisome is a major determinant of tumorigenicity in multiple organ sites and shows organ specificity (41), but outside of this report and the MET study, we have not identified any documentation of matrisomal changes in keratinocytes transformed by oncogenic RAS. These new results suggest that cell-autonomous modification of matrisomal components by RAS activation is an unexplored effector pathway for RAS-mediated tumor formation.

Increased oncogenic RAS signal strength increases gene expression of essential integrins

While remodeling of the matrisome was exclusively connected to tumor formation, the double *Ras* mutants and K mutant elevated the expression of essential integrin components α3, α6, and β1 integrins. Along with β4 integrin, these receptors bind to laminin components in the basement membrane and are essential for basal cell attachment to the basement membrane and to neighboring keratinocytes. It has been reported that α3β1 is essential for the formation and maintenance of skin papillomas *in vivo* and may represent a critical component of the RAS repertoire of changes needed for tumor formation in skin (42,43). Similarly, expression of α6β4 integrin is essential for keratinocyte attachment to substrates and a critical indicator of papilloma progression (44,45). Together, these integrins may enhance attachment to laminins in the incipient tumor microenvironment *in vivo* or in the wound bed in the orthograft assay to facilitate tumor formation.

The requirements for tumor formation in orthografts reflects *de novo* tumor formation

Gene dosage requirements have been well documented for *de novo* skin tumor development in transgenic and knock-in models. Expression of $Hras^{G12V}$ in transgenic mice produces multiple developmental anomalies and early mortality but surviving adults develop spontaneous skin papillomas, but only in homozygote adults (46). Additionally, two mutant alleles are required to produce an initiated phenotype when *LSL-*$Hras^{G12V}$ mice are crossed with K14-Cre transgenic mice (47). A single $Hras^{G12V}$ mutant allele is unable to drive tumorigenesis in the skin using K15-, Lgr5-, or Lgr6-Cre to drive activation (21). In contrast, papillomas form in mice harboring a single mutant $Kras^{G12D}$ allele (48–51) after crossing with skin-targeted transgenic Cre, a phenotype exacerbated by the addition of gain-of-function mutant $p53^{R172H}$ (52). Unfortunately, the genetic background of the mice employed in these studies is not always obvious. Thus, the specific *Ras* mutation, the particular H or K allele, the genetic background of the host, and the number of mutant copies all conspire to support tumor formation (48). The suppressive or enhancing function of a WT *Ras* allele has also been a consideration in tumor formation. For example, a WT *Kras* allele cooperates with mutant *Hras* to form papillomas in carcinogen-painted skin, perhaps explaining the co-amplification of chromosome 6 (*Kras*) and 7 (*Hras*) during papilloma progression (53). Similarly, the loss of one WT *Hras* allele reduces carcinogen-painted skin tumor burden by half, while 83% of papillomas erupting on $Hras^{KO/KO}$ mice harbor activating mutations in *Kras* (54). In our study, a mutant *Kras* allele reduced the expression of the WT *Hras* allele and slightly reduced protein levels, possibly reducing a signal needed for tumor formation that was overcome by the expression of two oncogenic alleles.

Increasing oncogenic RAS signal strength in single mutants restores tumorigenicity

We confirmed that several tumor initiation markers (*Areg*, *Krt1*, *Krt8*, *Krt10*, and *Cxcl1*) that characterize keratinocytes transformed by *v-*Ras^{Ha} are similarly induced by endogenous *Ras* mutant alleles. A single *Hras* allele produced a weak signal, with low MAPK activity, reduced activation of AP-1, low expression of initiation markers, and transcriptional profiles most similar to WT keratinocytes. Such cells were unable to prevent senescence or sustain growth under differentiating culture conditions, analogous to papillomas that regress upon withdrawal of tumor promoters *in vivo* (4). This may partially explain the need for tumor promotion *in vivo* or other processes for signal amplification such as gene duplication or chromosome amplification in *Hras*-driven tumors. Indeed, we found that tumor formation was restored when signal strength deficiencies were reversed via BRAF inhibitor treatment, which enhances MAPK activity by increasing the association of HRAS with ARAF and CRAF (36). The restoration of tumor growth by the BRAF inhibitor in this study recapitulates the rapid eruption of benign skin tumors with *Hras* mutations in human patients treated with BRAF inhibitors for other cancers (55).

When we developed the orthograft model, we envisioned that the capacity to form papillomas was a cell-autonomous property of the donor tumor cells (56,57). In the current study, K keratinocytes produced all the biochemical and molecular parameters associated with tumor formation but did not form tumors. We can now attribute this to cell-autonomous factors in the C57BL/6 genetic background that modifiy tumor-forming ability despite the expression of many transformed attributes. The C57BL/6 genetic background is well known to be skin tumor-repressive, a feature often attributed to its resistance to tumor promotion (37,38,57). By backcrossing to the FVB/N background for only three generations, the ability of keratinocytes bearing a single mutant K allele to form tumors was restored. Thus, cell-autonomous genetic modifiers alter tumorigenicity, which has implications for tumor susceptibility in patients carrying *Ras* mutations.

This is the first study to define the remodeled matrisome as a common feature of *Ras*-driven tumorigenesis in mouse keratinocytes. Further, we show that *Ras* output can be modified by the number of mutant alleles, with two being required for tumor formation, but this can be circumvented by increasing signal strength in single H mutants via BRAF inhibition and transferring single K mutants to a permissive genetic background. Together, these data, gathered through modifying *Ras* gene dosage and signal strength, have revealed nuances of RAS transforming activity in keratinocytes and brought new insight to understanding mouse skin carcinogenesis at the cellular level.

Supplementary material

Supplementary data are available at *Carcinogenesis* online.

Funding

This work was funded by the intramural program of the Center for Cancer Research of the National Cancer Institute under ZIA BC 004504.

Acknowledgements

The authors thank Marta Custer and Susan Walters for the mouse colonies care, Mark Simpson, and Jennifer Dwyer from the Molecular Pathology Unit for their help with tissue slide scanning and the NCI Center for Cancer Research Genomics Core for assistance with the digital droplet PCR.

Conflict of Interest Statement

The authors have declared that no conflict of interest exists.

Data Availability Statement

The data underlying this article are available in the article and in its online supplementary material.

References

1. McCreery, M.Q. et al. (2017) Chemical carcinogenesis models of cancer: back to the future. *Ann. Rev. Cancer Biol.*, 1, 295–312.
2. Roop, D.R. et al. (1986) An activated Harvey ras oncogene produces benign tumours on mouse epidermal tissue. *Nature*, 323, 822–824.
3. Brown, K. et al. (1986) v-ras genes from Harvey and BALB murine sarcoma viruses can act as initiators of two stage mouse skin carcinogenesis. *Cell*, 46, 447–456.
4. Burns, F.J. et al. (1976) Regression kinetics of mouse skin papillomas. *Cancer Res.*, 36, 1422–1427.
5. Aldaz, C.M. et al. (1991) Promoter independence as a feature of most skin papillomas in SENCAR mice. *Cancer Res.*, 51, 1045–1050.
6. Pelling, J.C. et al. (1986) Elevated expression of Ha-ras is an early event in two-stage skin carcinogenesis in SENCAR mice. *Carcinogenesis*, 7, 1599–1602.
7. Aldaz, C.M. et al. (1989) Sequential trisomization of chromosomes 6 and 7 in mouse skin premalignant lesions. *Mol. Carcinog.*, 2, 22–26.
8. Quintanilla, M. et al. (1986) Carcinogen-specific mutation and amplification of Ha-ras during mouse skin carcinogenesis. *Nature*, 322, 78–80.
9. Rehman, I. et al. (2000) Frequent codon 12 Ki-ras mutations in mouse skin tumors initiated by *N*-methyl-*N*′-nitro-*N*-nitrosoguanidine and promoted by mezerein. *Mol. Carcinog.*, 27, 298–307.
10. Megosh, L. et al. (1998) Analysis of ras gene mutational spectra in epidermal papillomas from K6/ODC transgenic mice. *Mol. Carcinog.*, 22, 145–149.
11. Cataisson, C. et al. (2016) MET signaling in keratinocytes activates EGFR and initiates squamous carcinogenesis. *Sci Signal.*, 9, ra62.
12. Simanshu, D.K. et al. (2017) RAS proteins and their regulators in human disease. *Cell*, 170, 17–33.
13. Hobbs, G.A. et al. (2016) RAS isoforms and mutations in cancer at a glance. *J. Cell Sci.*, 129, 1287–1292.
14. Potenza, N. et al. (2005) Replacement of K-Ras with H-Ras supports normal embryonic development despite inducing cardiovascular pathology in adult mice. *EMBO Rep.*, 6, 432–437.
15. Drosten, M. et al. (2017) H-Ras and K-Ras oncoproteins induce different tumor spectra when driven by the same regulatory sequences. *Cancer Res.*, 77, 707–718.
16. Li, S. et al. (2018) A model for RAS mutation patterns in cancers: finding the sweet spot. *Nat. Rev. Cancer*, 18, 767–777.
17. Bailleul, B. et al. (1990) Skin hyperkeratosis and papilloma formation in transgenic mice expressing a ras oncogene from a suprabasal keratin promoter. *Cell*, 62, 697–708.
18. Greenhalgh, D.A. et al. (1993) Induction of epidermal hyperplasia, hyperkeratosis, and papillomas in transgenic mice by a targeted v-Ha-ras oncogene. *Mol. Carcinog.*, 7, 99–110.
19. Jackson, E.L. et al. (2001) Analysis of lung tumor initiation and progression using conditional expression of oncogenic K-ras. *Genes Dev.*, 15, 3243–3248.
20. Tuveson, D.A. et al. (2004) Endogenous oncogenic K-ras(G12D) stimulates proliferation and widespread neoplastic and developmental defects. *Cancer Cell*, 5, 375–387.
21. Lowry, W.E. et al. (2016) Exploiting mouse models to study Ras-induced cutaneous squamous cell carcinoma. *J. Invest. Dermatol.*, 136, 1543–1548.
22. Hansen, L.A. et al. (2000) The epidermal growth factor receptor is required to maintain the proliferative population in the basal compartment of epidermal tumors. *Cancer Res.*, 60, 3328–3332.
23. Cataisson, C. et al. (2009) Inducible cutaneous inflammation reveals a protumorigenic role for keratinocyte CXCR2 in skin carcinogenesis. *Cancer Res.*, 69, 319–328.
24. Cataisson, C. et al. (2012) IL-1R-MyD88 signaling in keratinocyte transformation and carcinogenesis. *J. Exp. Med.*, 209, 1689–1702.
25. Platt, R.J. et al. (2014) CRISPR-Cas9 knockin mice for genome editing and cancer modeling. *Cell*, 159, 440–455.
26. Lichti, U. et al. (2008) Isolation and short-term culture of primary keratinocytes, hair follicle populations and dermal cells from newborn mice and keratinocytes from adult mice for in vitro analysis and for grafting to immunodeficient mice. *Nat. Protoc.*, 3, 799–810.
27. Lee, A.J. et al. (2021) RAS induced senescence of skin keratinocytes is mediated through Rho-associated protein kinase (ROCK). *Mol. Carcinog.*, 60, 799–812.
28. Ritchie, M.E. et al. (2015) limma powers differential expression analyses for RNA-sequencing and microarray studies. *Nucleic Acids Res.*, 43, e47.
29. Yuspa, S.H. et al. (1989) Expression of murine epidermal differentiation markers is tightly regulated by restricted extracellular calcium concentrations in vitro. *J. Cell Biol.*, 109, 1207–1217.
30. Dlugosz, A.A. et al. (1995) Autocrine transforming growth factor à is dispensible for v-ras Ha-induced epidermal neoplasia: potential involvement of alternate epidermal growth factor receptor ligands. *Cancer Res.*, 55, 1883–1893.
31. Ha, L. et al. (2011) Dysregulated DeltaNp63alpha inhibits expression of Ink4a/arf, blocks senescence, and promotes malignant conversion of keratinocytes. *PLoS One*, 6, e21877.
32. Cataisson, C. et al. (2019) T-Cell Deletion of MyD88 Connects IL17 and IkappaBzeta to RAS Oncogenesis. *Mol. Cancer Res.*, 17, 1759–1773.

33. Rutberg, S.E. et al. (2000) Activator protein 1 transcription factors are fundamental to v-ras Ha—induced changes in gene expression in neoplastic keratinocytes. *Cancer Res.*, 60, 6332–6338.
34. Larcher, F. et al. (1992) Aberrant expression of the simple epithelial type II keratin 8 by mouse skin carcinomas but not papillomas. *Mol. Carcinog.*, 6, 112–121.
35. Naba, A. et al. (2012) The matrisome: in silico definition and in vivo characterization by proteomics of normal and tumor extracellular matrices. *Mol. Cell. Proteom.*, 11, M111–014647.
36. Terrell, E.M., et al. (2019) Distinct binding preferences between Ras and Raf family members and the impact on oncogenic Ras signaling. *Mol Cell*, 76, 872-884.e5
37. Abel, E.L. et al. (2009) Multi-stage chemical carcinogenesis in mouse skin: fundamentals and applications. *Nat. Protoc.*, 4, 1350–1362.
38. Woodworth, C.D. et al. (2004) Strain-dependent differences in malignant conversion of mouse skin tumors is an inherent property of the epidermal keratinocyte. *Carcinogenesis*, 25, 1771–1778.
39. Bremner, R. et al. (1990) Genetic changes in skin tumor progression: correlation between presence of a mutant ras gene and loss of heterozygosity on mouse chromosome 7. *Cell*, 61, 407–417.
40. Rudzka, D.A. et al. (2021) Selection of established tumour cells through narrow diameter micropores enriches for elevated Ras/Raf/MEK/ERK MAPK signalling and enhanced tumour growth. *Small GTPases*, 12, 294–310.
41. Rafaeva, M. et al. (2020) Framing cancer progression: influence of the organ- and tumour-specific matrisome. *FEBS J.*, 287, 1454–1477.
42. Sachs, N. et al. (2012) Loss of integrin alpha3 prevents skin tumor formation by promoting epidermal turnover and depletion of slow-cycling cells. *Proc. Natl. Acad. Sci. U.S.A.*, 109, 21468–21473.
43. Ramovs, V. et al. (2021) Integrin alpha3beta1 is a key regulator of several protumorigenic pathways during skin carcinogenesis. *J. Invest. Dermatol.*, 141, 732–741 e6.
44. Tennenbaum, T. et al. (1993) The suprabasal expression of à6á4 integrin is associated with a high risk for malignant progression in mouse skin carcinogenesis. *Cancer Res.*, 53, 4803–4810.
45. Alt, A. et al. (2001) Protein kinase Cdelta-mediated phosphorylation of alpha6beta4 is associated with reduced integrin localization to the hemidesmosome and decreased keratinocyte attachment. *Cancer Res.*, 61, 4591–4598.
46. Chen, X. et al. (2009) Endogenous expression of Hras(G12V) induces developmental defects and neoplasms with copy number imbalances of the oncogene. *Proc. Natl. Acad. Sci. U.S.A.*, 106, 7979–7984.
47. Beronja, S. et al. (2013) RNAi screens in mice identify physiological regulators of oncogenic growth. *Nature*, 501, 185–190.
48. Lapouge, G. et al. (2011) Identifying the cellular origin of squamous skin tumors. *Proc. Natl. Acad. Sci. U.S.A.*, 108, 7431–7436.
49. White, A.C. et al. (2011) Defining the origins of Ras/p53-mediated squamous cell carcinoma. *Proc. Natl. Acad. Sci. U.S.A.*, 108, 7425–7430.
50. Mukhopadhyay, A. et al. (2011) Activated Kras alters epidermal homeostasis of mouse skin, resulting in redundant skin and defective hair cycling. *J. Invest. Dermatol.*, 131, 311–319.
51. White, A.C. et al. (2014) Stem cell quiescence acts as a tumour suppressor in squamous tumours. *Nat. Cell Biol.*, 16, 99–107.
52. Caulin, C. et al. (2007) An inducible mouse model for skin cancer reveals distinct roles for gain- and loss-of-function p53 mutations. *J. Clin. Invest.*, 117, 1893–1901.
53. Aldaz, C.M. et al. (1986) Cytogenetic evidence for gene amplification in mouse skin carcinogenesis. *Cancer Res.*, 46, 3565–3568.
54. To, M.D. et al. (2013) Interactions between wild-type and mutant Ras genes in lung and skin carcinogenesis. *Oncogene*, 32, 4028–4033.
55. Su, F. et al. (2012) RAS mutations in cutaneous squamous-cell carcinomas in patients treated with BRAF inhibitors. *N. Engl. J. Med.*, 366, 207–215.
56. Balmain, A. et al. (2014) Milestones in skin carcinogenesis: the biology of multistage carcinogenesis. *J. Invest. Dermatol.*, 134, E2–E7.
57. Shen, J. et al. (2012) Proteomic and pathway analyses reveal a network of inflammatory genes associated with differences in skin tumor promotion susceptibility in DBA/2 and C57BL/6 mice. *Carcinogenesis*, 33, 2208–2219.